

Highlights

Tire Dimensionless Numbers for Analysis of Tire Characteristics and Intelligent Tire Signals

Dasol Jeong, Seibum B. Choi, Jonghyup Lee, Mintae Kim, Hojong Lee

- Proposal for tire model dimensionless numbers through flexible ring tire model
- Analysis of tire vibration characteristics through intelligent tires using FFT(fast Fourier transform).
- Estimation of tire model dimensionless numbers through intelligent tire sensors.
- Analysis of tire characteristics through tire model dimensionless numbers.

Tire Dimensionless Numbers for Analysis of Tire Characteristics and Intelligent Tire Signals

Dasol Jeong^a, Seibum B. Choi^{a,*}, Jonghyup Lee^a, Mintae Kim^b, Hojong Lee^b

^a*Department of Mechanical Engineering, KAIST, 291 Daehak-ro Yuseong-gu, Daejeon, 34141, Republic of Korea*

^b*HANKOOK TIRE CO. LTD, Daejeon 34127, Republic of Korea*

Abstract

It is essential to understand and analyze the characteristics of the tire. This paper focuses on analyzing tire characteristics using intelligent tires based on physical tire models. The flexible ring tire model has been selected as the tire model. The flexible ring tire model is analyzed and simplified based on modal analysis. Four tire dimensionless numbers have been proposed to represent tire characteristics using the Buckingham theorem. Tire dimensionless numbers were estimated using intelligent tire sensor signals. The estimation algorithm was designed based on the standing wave characteristics of the tire. The proposed estimation algorithm has been validated through experiments on various tire conditions. The physical correlation between the estimated tire dimensionless numbers and the tire state dimensionless numbers were analyzed. The experimental results verify the physical meaning and estimation performance of the proposed tire dimensionless numbers.

Keywords: Intelligent tires, flexible ring tire model, Buckingham theorem, tire dimensionless numbers, tire condition dimensionless numbers, fast Fourier transform(FFT)

1. Introduction

Tires are the only elements in the vehicle that are in contact with the road surface. The forces and moments between the tire and the road surface play a major role in the acceleration, deceleration, and steering of the vehicle. Estimation of tire states such as tire load, pressure, and wear is an important study in vehicle control/vehicle state estimation [1] and autonomous vehicles [2], [3]. Also, analyzing tire characteristics such as tire sidewall stiffness [4], contact property [5], and rolling resistance [6] is an important study in the measurement field.

Intelligent tires are new concept tires with additional sensors inside the tires. Intelligent tires have the advantage of being able to estimate tire states and characteristics that are very important for vehicle control but hard to estimate. Intelligent tires are classified into two types, one using acceleration sensors [7], [8] and the other using strain sensors [9]. Acceleration sensors are more sensitive to noise than strain sensors and require advanced signal processing techniques. However, acceleration sensors have the advantages of compact size, high-energy efficiency, and low cost [10]. Therefore, in this study, acceleration sensors are selected and attached to the tire inner liner for durability.

The signals of each axis of the acceleration sensors of the intelligent tires are shown in Fig. 1. Each figure represents the radial, longitudinal, and lateral accelerations measured through acceleration sensors of intelligent tires. The acceleration signals inside tires are changed by various tire states such as tire load, pressure, wear, and road surface. Also, acceleration sensor signals are changed by tire characteristics such as tire radius, bending stiffness, and sidewall stiffness. It means that the intelligent tire sensor signal includes tire states and tire characteristics.

In recent years, studies on estimation of tire states such as wear [11], [12], load [13], [14], [15] road surface [16], [17], slip angle [18], [19], traction/braking force [20] through intelligent tires have been studied. The estimated tire information affects the improvement of ride comfort, safety, and driving ability of the vehicle [21]. However, most

*Corresponding author

Email address: sbchoi@kaist.ac.kr (Seibum B. Choi)

Nomenclature

Dimensionless numbers

B_s	Bending stiffness number	-
C_w	Contact width number	-
P_n	Pressure number	-
R_s	Radial stiffness number	-
T_m	Modal tire model number	-
T_s	Tangential stiffness number	-
W_n	Wear number	-

Flexible ring tire model parameters

Ω	Angular velocity of the tire	rad/s
ρ	Density of the ring material	kg/m ³
σ_θ^0	Initial normal stress	N/m ²
θ_f	Front contact angle	rad
θ_r	Rear contact angle	rad
A	Cross section area of the ring	m ²
b	Width of the ring	m
E	Young's modulus of the ring	N/m ²
h	Thickness of the ring	m
h_0	Initial thickness of the ring for the new tire	m
I	Inertia moment of the cross section of the ring	m ⁴
k_v	Tangential stiffness of the sidewall	N/m ²
k_w	Radial stiffness of the sidewall	N/m ²
p_o	Inflation pressure of the tire	N/m ²
q_v	External force acting on the ring tangentially	N/m
q_w	External force acting on the ring radially	N/m
R	Mean radius of the sidewall	m
v	Tangential displacement of the ring	m
w	Radial displacement of the ring	m

Modal analysis parameters

γ_n	Parameter that describes an asymmetry of the tire	rad
A_n	Modal tire model	m ² /N
c_n	Parameter that describes the damping effect of the tire	Ns/m ²
F_n	Modal tire force	N/m
g_n	Parameter that acts as a damper in the modal tire model	Ns/m ²
k_n	Parameter that acts as a spring in the modal tire model	N/m ²
m_n	Parameter that acts as a mass in the modal tire model	kg/m

previous studies have been based on data-based phenomenon observations. It implies weakness in generality and robustness. Recently, to overcome this, the estimation of tire vertical and longitudinal forces using a physical tire model has been studied [22]. In this way, tire characteristic analysis is essential to improving intelligent tire research.

Moreover, tire characteristics are an important criterion for determining tire performance and property. In the field of measurements and instrumentation, characteristics of tire-road contact [23], [5], rolling resistance [24], [6], tire stiffness [4], [25], and the influence of tire pressure on vehicle dynamics [21] were studied. Previous researches are not suitable for this study for the following reasons: The first is analysis offline. Changing characteristics such as wear stiffness cannot be analyzed. The second is time-consuming. A calibration effort is accompanied by each tire. In this study, we propose an algorithm for analyzing tire characteristics through intelligent tires. It has the advantage

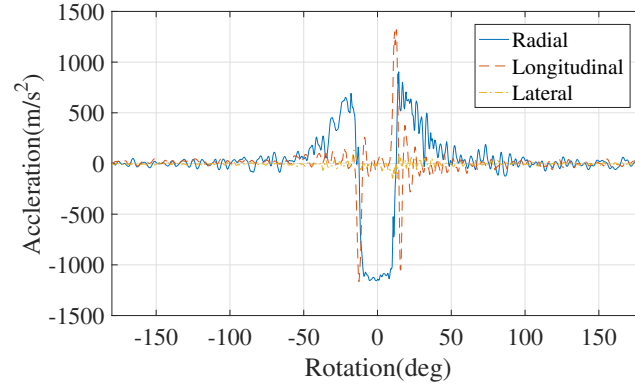


Figure 1: Three-axis acceleration signal on intelligent tires with acceleration sensor

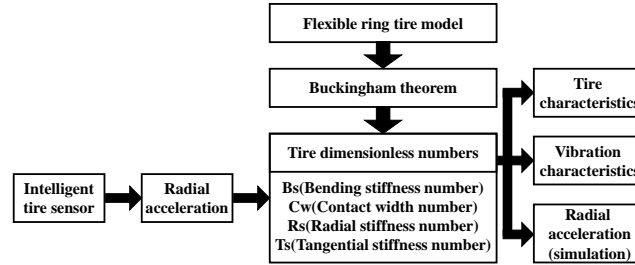


Figure 2: Schematic of proposed algorithm

of real-time characteristic analysis and less time-consuming. The proposed algorithm was verified through a physical tire model.

Several physical tire models have been considered to combine with intelligent tires. Many physical tire models have been studied to analyze the characteristics of tires. The following models can be considered: the tire model for determining the contact properties of tires [26], the non-pneumatic tire model [27], the motorcycle tire model [28], the belted tire model for trucks and buses [29], and the flexible ring tire model [30]. The flexible ring tire model was similar to the actual tire, and a good representation of the tire characteristics. A lot of research has been studied through the flexible ring tire model: contact properties of tires [31], tire model analysis through physical assumptions [32], and comparison with actual tire deformation [33]. Also, the flexible ring tire model has the advantage of describing the deformation of the attachment position of the intelligent tire sensors. For these reasons, the flexible ring tire model was used to analyze intelligent tire sensor signals.

The flexible ring tire model was analyzed using many tire model parameters. In this paper, the flexible ring tire model is simplified through physical assumptions. Through model simplification, tire dimensionless numbers representing the characteristics of the tire were defined. The tire dimensionless numbers were estimated through the intelligent tire sensor signals. The schematic of the proposed algorithm is shown in Fig. 2. In conclusion, tire characteristics can be effectively analyzed through the proposed tire dimensionless estimation algorithm.

The rest of the paper is organized as follows. Section 2 introduces intelligent tire sensors and experimental environments. In section 3, the flexible ring tire model and modal analysis are introduced. In section 4, tire dimensionless numbers are proposed. In section 5 an estimation algorithm of tire dimensionless numbers is proposed through the model simplification. Experimental validation is presented in section 6, and conclusions are provided in section 7.

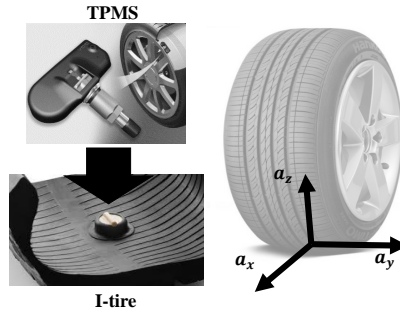


Figure 3: Acceleration sensor attachment location



Figure 4: Flat trac

2. TEST ENVIRONMENT

In this paper, the acceleration sensors were selected as intelligent tire sensors. The acceleration sensors measure the radial acceleration. The shape of the measured radial acceleration signal is shown in Fig. 1. The measurement range of the sensor is $-2000g$ to $+2000g$ and the sampling rate is 9600Hz . The sensor was attached to the inner liner of the tire for durability. Also, the attached position is the center of the lateral reference of the tire as shown in Fig. 3. The tires selected were Hankook H426 245R15 / 25 tires. This is a four-season tire that is common. The Flat trac was used for intelligent tire tests. The Flat trac, shown in Fig. 4, has the advantage of being able to test easily by changing various tire conditions. Radial acceleration signals of intelligent tires were collected under various conditions (load, speed, pressure, wear). The conditions of the tire are shown in Table. 1.

Table 1: Experimental conditions

Variable	Condition
Load	40%, 100%, 1600% (100%=5000N)
Pressure	1.7bar, 2.1bar, 2.5bar
Wear	0mm, 2.9mm, 6.4mm (0mm: new tire)
Velocity	65km/h

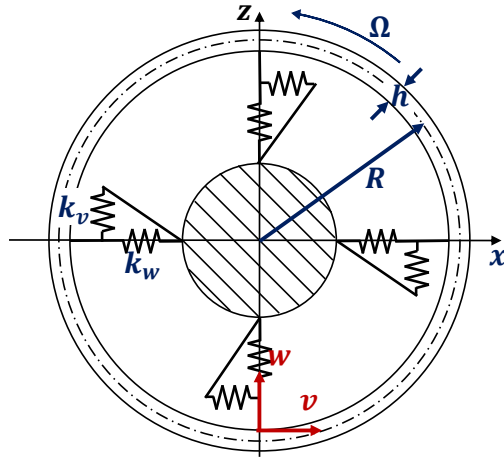


Figure 5: Flexible ring tire model

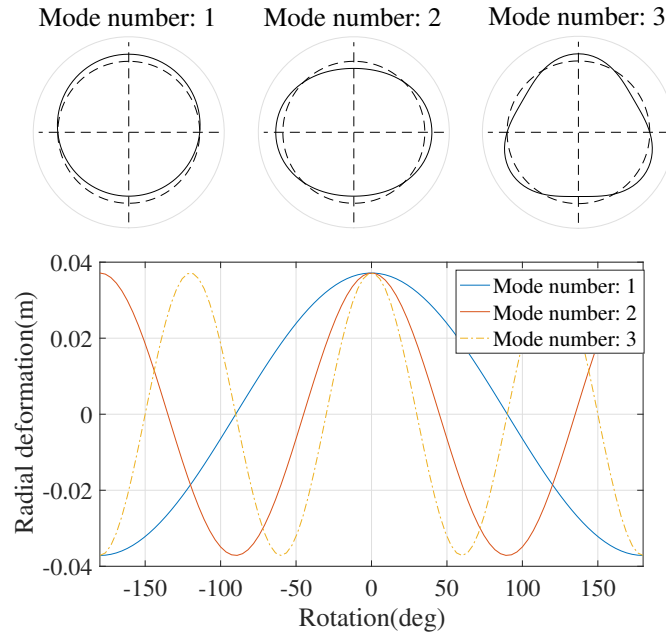


Figure 6: Standing wave characteristics according to mode number

3. FLEXIBLE RING TIRE MODEL

The flexible ring tire model consists of the tread band, the sidewall, and the wheel as shown in Fig. 5 [30]. And many tire model parameters and states were used to describe the tire dynamics. The most important states are radial deformation of the ring (w) and tangential deformation of the ring (v). These are the states that represent the deformation of radial and tangential directions inside the tire. The position where the states are defined corresponds to the sensor attachment position of the intelligent tire. For this reason, the flexible ring tire model has advantages in analyzing intelligent tire sensor signals.

The flexible ring tire model is analyzed by an energy analysis of tire deformation. Strain energy, elastic energy of the foundation, kinetic energy, and virtual work of external force are used. Each energy is expressed by the following equations [30]. σ_{θ}^0 is the initial stress applied to the tread band of the tire, p_0 represents the pressure

- Strain energy

$$\begin{aligned}
S_1 &= b \int \int \left[\frac{1}{2} \sigma_\theta \epsilon_\theta + \sigma_\theta^0 \epsilon_\theta \right] R dy d\theta \\
&= \int \frac{1}{2} \left\{ 2\sigma_\theta^0 A \left(w + \frac{\partial v}{\partial \theta} \right) + \frac{\sigma_\theta^0 A}{R} \left(v - \frac{\partial w}{\partial \theta} \right)^2 + \frac{E}{R} \left[A \left(w + \frac{\partial v}{\partial \theta} \right)^2 + \frac{I}{R^2} \left(\frac{\partial v}{\partial \theta} - \frac{\partial^2 w}{\partial \theta^2} \right) \right] \right\} d\theta
\end{aligned} \quad (1)$$

- Elastic energy of the foundation

$$S_2 = \int \frac{1}{2} (k_v v^2 + k_w w^2) R d\theta \quad (2)$$

- Kinetic energy

$$T_1 = \int \frac{1}{2} \rho A R \left[(\dot{w} - v\Omega)^2 + \left(\dot{v} + (R+w)\Omega^2 \right)^2 \right] \quad (3)$$

- Virtual work of external forces

$$\delta E_1 = \int [q_w \delta v] R d\theta \quad (4)$$

$$\delta E_2 = \int p_0 b \left[\left(1 + \frac{1}{R} (w + \frac{\partial v}{\partial \theta}) \right) \delta w - \frac{1}{R} \left(\frac{\partial w}{\partial \theta} - v \right) \delta v \right] R d\theta \quad (5)$$

In the above equations, dot(·) is the derivative with respect to time. Each energy is combined through Hamilton's principle. The governing equation of the flexible ring tire model is obtained as follows:

$$\frac{EI}{R^4} \left(\frac{\partial^4 w}{\partial \theta^4} - \frac{\partial^3 v}{\partial \theta^3} \right) + \frac{EA}{R^2} \left(w + \frac{\partial v}{\partial \theta} \right) + \frac{\sigma_\theta^0 A}{R^2} \left(\frac{\partial v}{\partial \theta} - \frac{\partial^2 w}{\partial \theta^2} \right) + k_w w + \rho A (\ddot{w} - 2\Omega \dot{v} - \Omega^2 w) - \frac{p_0 b}{R} \left(\frac{\partial v}{\partial \theta} + w \right) = q_w \quad (6)$$

$$\frac{EI}{R^4} \left(\frac{\partial^3 w}{\partial \theta^3} - \frac{\partial^2 v}{\partial \theta^2} \right) + \frac{EA}{R^2} \left(\frac{\partial w}{\partial \theta} + \frac{\partial^2 v}{\partial \theta^2} \right) + \frac{\sigma_\theta^0 A}{R^2} \left(v - \frac{\partial w}{\partial \theta} \right) + k_v v + \rho A (\ddot{v} + 2\Omega \dot{w} - \Omega^2 v) + \frac{p_0 b}{R} \left(\frac{\partial w}{\partial \theta} - v \right) = q_v \quad (7)$$

(6) and (7) are well describing the dynamics of the radial and longitudinal deformation of the ring. However, it has a disadvantage in the complexity of the governing equation. In a previous study [30], modal analysis was used to solve the governing equations. Modal analysis is a method of analyzing tire deformation as the sum of standing waves. This means that the deformation of the tire consists of standing waves as shown in Fig. 6. This is reasonable from a physical point of view because the deformation at the end of the tire must be continuous. And only standing waves satisfy this condition.

The modal analysis was verified by the intelligent tire sensor signal. The radial acceleration for several rotations measured by intelligent tires is shown in Fig. 7 (a). The result of analyzing the axial acceleration through fast Fourier transform(FFT) is shown in Fig. 7 (b). As shown in Fig. 7 (b), the amplitude is maximum when the value of the x-axis is an integer. This means that the standing wave vibration of the tire dominates the tire vibration. By FFT analysis, the use of modal analysis in the analysis of flexible ring tire models is reasonable both physically and experimentally. Through modal analysis and some assumptions, the radial deformation is expressed as follows [30]:

- In-extensibility assumption: The central circumference length of the tire ring does not change.

$$w = -\frac{\partial v}{\partial \theta} \quad (8)$$

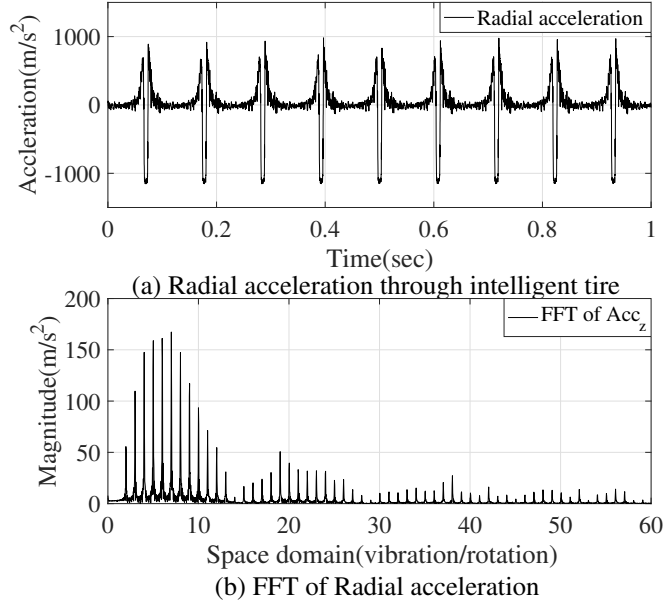


Figure 7: Experimental verification of modal analysis

- Free-rolling assumption: The tire rotates in steady-state.

$$\frac{\partial w}{\partial \theta} = 0, \frac{d^2 \theta}{dt^2} = 0 \quad (9)$$

- Radial deformation of the ring (w)

$$w(\theta) = \sum_{n=0}^{\infty} A_n F_n \quad (10)$$

where n = mode number

- Modal tire model(A_n)

$$A_n = -\frac{n^2}{\pi} \frac{1}{\sqrt{[k_n - m_n(n\Omega)^2 - g_n(n\Omega)]^2 + [c_n(n\Omega)]^2}} \quad (11)$$

where $m_n = \rho A(1 + n^2)$, $g_n = -4\rho A n \Omega$, $c_n = c_v + c_w n^2$

$$k_n = \left(\frac{EI}{R^4} n^2 + \frac{\sigma_\theta^0}{R^2} \right) (1 - n^2)^2 - \frac{p_0 b}{R} (1 - n^2) + k_v + k_w n^2 - \rho A (1 + n^2) \Omega^2$$

- Modal tire force(F_n)

$$F_n = \alpha_n \cos(\theta - \gamma_n) + \beta_n \sin(\theta - \gamma_n) \quad (12)$$

$$\text{where } \alpha_n = \int_{\theta_f}^{\theta_r} q_w(\theta) \cos(n\theta) d\theta, \beta_n = \int_{\theta_f}^{\theta_r} q_w(\theta) \sin(n\theta) d\theta, n\gamma_n = \tan^{-1} \left(\frac{c_n(n\Omega)}{k_n - m_n(n\Omega)^2 - g_n(n\Omega)} \right)$$

Table 2: Dimensions of each variable using the mass-length time(MLT) system

Variable	A_n	EI	p_0	k_w	k_v	b	R
Dimension	$ML^{-1}T^{-2}$	ML^3T^{-2}	$ML^{-1}T^{-2}$	$ML^{-1}T^{-2}$	$ML^{-1}T^{-2}$	L	L

4. SIMPLIFICATION OF THE FLEXIBLE RING TIRE MODEL

In this section, tire dimensionless numbers are defined through the simplification of the flexible ring tire model. (10) describes the deformation of the ring in detail, but it has the disadvantage of complexity. To simplify the modal tire model and modal tire force, the no-damping effect assumption was used. This assumption means that there is no damping effect inside the tire ($c_n = 0$). Since there is no damping effect inside the tire, the overall deformation of the tire is symmetrical to the left and right. As a result, tire deformation is simplified and four tire dimensionless numbers are defined. Simplified modal tire model and modal tire force are introduced in section 4.1 and section 4.2

4.1. Simplification of Modal Tire Model and Proposing to Tire Dimensionless Numbers

In this section, the modal tire model is simplified and the tire dimensionless numbers are proposed. Using the no-damping effect assumption, the modal tire model can be expressed as follows:

$$A_n(\text{simplified modal tire model}) = -\frac{n^2}{\pi} \times \frac{R^4}{EI(n^6 - 2n^4 + n^2) + bR^3 p_0(n^4 - n^2) + k_w R^4 n^2 + k_v R^4} \quad (13)$$

Buckingham PI theorem [34] is used to define the tire dimensionless numbers.

- Buckingham PI theorem: m independent variables including n primary dimensions (length L , force N , time T , mass M , temperature K , etc.) can form $m - n$ dimensionless variables.

Based on the Buckingham PI theorem, $m = 7$ (modal tire model A_n , tire bending strength EI , tire pressure p_0 , tire sidewall radial stiffness k_w , tire sidewall tangential stiffness k_v , contact width b , and Tire radius R), and $n = 2$ (length L , force N). After that, tire radius R and tire pressure p_0 were selected as physical variables ($r = 2$). The dimensions of the variables based on the mass-length-time(MLT) system are shown in Table. 2.

For example, tire bending strength(EI) can be changed to the bending stiffness number(Bs) using dimensional analysis as follow:

$$Bs = \prod A(EI, (R, p_0)) = (EI)^a (R)^b (p_0)^c = (ML^3T^{-2})^a (L)^b (ML^{-1}T^{-2})^c = M^0 L^0 T^0 \quad (14)$$

Equate exponents:

$$a = 1, b = -4, c = -1 \quad (15)$$

Therefore, the bending stiffness number(Bs) is defined as follows:

$$Bs = \prod A(EI, (R, p_0)) = \frac{EI}{R^4 p_0} \quad (16)$$

In this way, the tire dimensionless numbers, the modal tire model number(Tm), the bending stiffness number(Bs), the contact width number(Cw), the radial stiffness number(Rs), and the tangential stiffness number(Ts), are defined as follows:

$$\begin{aligned} Tm &= \prod T(A_n, (R, p_0)) = A_n p_0, Bs = \prod A(EI, (R, p_0)) = \frac{EI}{R^4 p_0}, Cw = \prod B(b, (R, p_0)) = \frac{b}{R} \\ Rs &= \prod C(k_w, (R, p_0)) = \frac{k_w}{p_0}, Ts = \prod D(k_v, (R, p_0)) = \frac{k_v}{p_0} \end{aligned} \quad (17)$$

The following relationship can be confirmed through dimensional analysis.

$$Tm = f(Bs, Cw, Rs, Ts) \quad (18)$$

By simplifying and dimensional analysis, the simplified modal tire model can be represented by four tire dimensionless numbers as shown below.

$$A_n = -\frac{n^2}{\pi p_0} \times \frac{1}{Bs(n^6 - 2n^4 + n^2) + Cw(n^4 - n^2) + Rsn^2 + Ts} \quad (19)$$

$$\text{where } Bs \left(= \frac{EI}{R^4 p_0} = \frac{bEh^3}{12R^4 p_0} \right) : \frac{\text{Bending stiffness}}{\text{Inflation pressure}}, Cw \left(= \frac{b}{R} \right) : \frac{\text{Contact width}}{\text{Tire radius}}$$

$$Rs \left(= \frac{k_w}{p_0} \right) : \frac{\text{Radial stiffness of sidewall}}{\text{Inflation pressure}}, Ts \left(= \frac{k_v}{p_0} \right) : \frac{\text{Tangential stiffness of sidewall}}{\text{Inflation pressure}}$$

Each tire dimensionless number means: Bs is the bending stiffness divided by the tire radius and pressure, and is the factor for how well the tire bends. Cw is the contact width divided by the tire radius and is the factor for how wide the tire contacts the road surface. Rs is the ratio of the radial stiffness of the tire sidewalls to the pressure and Ts is the ratio of the tangential stiffness of the tire sidewalls to the pressure.

4.2. Simplification of Modal Tire Force for Each Mode of Standing Wave

The modal tire force is also simplified. Using the no-damping effect assumption, the modal tire force is expressed as follows:

$$n\gamma_n = \tan^{-1} \left(\frac{c_n(n\Omega)}{k_n - m_n(n\Omega)^2 - g_n(n\Omega)} \right) = 0 \quad (20)$$

In addition, the following assumptions were used for the simplicity of the analysis.

- Assumption: Normal force ($q_w(\theta)$) is distributed uniformly.

It means that when the tire contacts with the road surface, the normal force of the tire is uniform in all-region. Through these assumptions, the modal tire force is expressed as follows:

$$F_n = \alpha_n \cos n(\theta) \quad (21)$$

In the contact region, the sum of the normal force should be equal to the total tire load, and the normal force at both edges of the tire-road contact must be zero. Therefore, the following constraints are defined.

- Constraint 1:

$$R \int_{\theta_f}^{\theta_r} q_w(\theta) d\theta = Q_w, \text{ where, } Q_w = \text{Total tire load}$$

- Constraint 2: $q_w(\theta_f) = q_w(\theta_r) = 0$

The distribution of force can also be confirmed through Fig. 8, and q_w is expressed as follows:

$$q_w(\theta) = \frac{Q_w}{2R\theta_r} \quad (22)$$

In (22), tire load and contact angle can be estimated through intelligent tire sensor signals [7], [13], [15]. Finally, the modal tire force can be expressed as follows:

$$F_n = \frac{Q_w}{nR\theta_r} \sin n\theta_r \cos n\theta \quad (23)$$

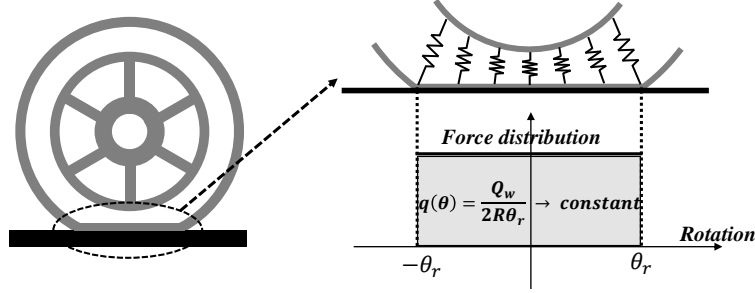


Figure 8: External force acting on ring radially

5. ESTIMATION OF TIRE DIMENSIONLESS NUMBERS USING INTELLIGENT TIRE SENSOR

In this section, the estimation algorithm of the tire dimensionless numbers based on intelligent tires is proposed. Through the simplification of the modal tire model and the modal tire force, the deformation of the ring is expressed as follows:

$$w(\theta) = \sum_{n=0}^{\text{inf}} A_n F_n \quad (24)$$

$$\text{where } n = \text{mode number, } A_n = -\frac{n^2}{\pi p_0} \times \frac{1}{Bs(n^6 - 2n^4 + n^2) + Cw(n^4 - n^2) + Rsn^2 + Ts}$$

$$F_n = \alpha_n \cos(n\theta) = \frac{Q_w}{nR\theta_r} \sin n\theta_r \cos n\theta$$

By differentiating the above equation twice over time using the free-rolling assumption as shown in (9), the radial acceleration inside the tire can be obtained as (25). The position where (25) is defined is the same as the sensor attachment position of the intelligent tire. Therefore, the left side of (25) can be directly measured by the intelligent tire sensor.

$$\ddot{w}(\theta) = -\Omega^2 \sum_{n=0}^{\text{inf}} n^2 \times A_n F_n \quad (25)$$

(25) consists of the Fourier series and consists only of the cosine component. By using the properties of the Fourier series, (25) can be expressed as follows:

$$\int_{-\pi}^{\pi} \ddot{w}(\theta) \frac{1}{\Omega^2} \cos(n\theta) d\theta = -\pi n^2 A_n \alpha_n \quad (26)$$

Substituting the simplified modal tire model and modal tire force, the following equation can be expressed as (27).

$$\frac{\int_{-\pi}^{\pi} \ddot{w}(\theta) \cos(n\theta) d\theta}{\pi \Omega^2} = -\frac{Q_w}{R\theta_r \pi p_0} \sin n\theta_r \times \frac{n^3}{Bs(n^6 - 2n^4 + n^2) + Cw(n^4 - n^2) + Rsn^2 + Ts} \quad (27)$$

Equation (27) represents the standing wave characteristic of the radial acceleration signal of the intelligent tires. Also, the left side of (27) consists of measurements. The right side shows the standing wave characteristics of the radial acceleration of the tire ring expressed by the flexible ring tire model. The right side consists of the tire states (Q_w , R , θ_r , and n) and the unknown tire dimensionless numbers (Bs , Cw , Rs , and Ts). Of the tire states, R and n are known and Q_w and θ_r can be estimated using intelligent tires [15]. Finally, the tire dimensionless numbers can be

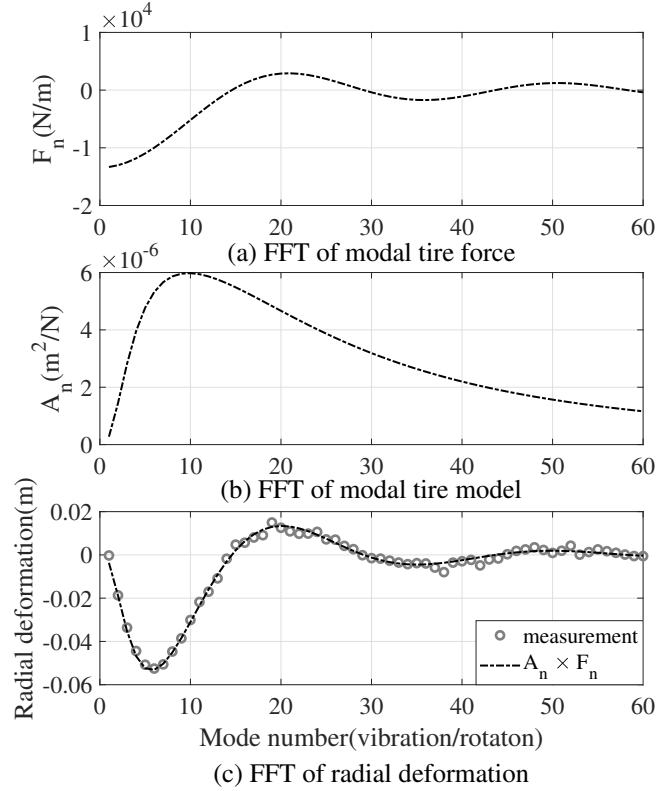


Figure 9: Estimation algorithm of tire dimensionless numbers

estimated by fitting the right side of (27) to the left side of (27) as shown in Fig. 9. Further, according to the previous study [30], it uses mode numbers from 1 to 60.

Modal tire force, modal tire model, and modal radial deformation are shown in Fig. 9. The x-axis of each graph represents the standing wave mode number. Fig. 9 (a) shows the simplified modal tire force. Fig. 9 (b) shows the simplified modal tire model through the four tire dimensionless numbers. The modal tire model value acts as the transfer function of the system. The in-tire radial deformation magnitude for each standing wave is shown in Fig. 9 (c). In Fig. 9 (c), the dotted line represents the value measured by the intelligent tire sensor, and the solid line represents the value estimated through the flexible ring tire model using tire dimensionless numbers. The estimation strategy is to estimate tire dimensionless numbers by fitting the solid line to the dotted line as shown in Fig. 9 (c). In conclusion, the tire model dimensionless numbers are estimated as follows:

$$J = \sum_{n=1}^{60} \left(\frac{\int_{-\pi}^{\pi} \ddot{w}(\theta) \cos(n\theta) d\theta}{\pi \Omega^2} - \left(-\frac{Q_w}{R\theta_r \pi p_0} \sin n\theta_r \times \frac{n^3}{Bs(n^6 - 2n^4 + n^2) + Cw(n^4 - n^2) + Rsn^2 + Ts} \right) \right)^2 \quad (28)$$

$$\hat{B}s, \hat{C}w, \hat{R}s, \hat{T}s = \operatorname{argmin}_{Bs, Cw, Rs, Ts} (J) \quad (29)$$

Fig. 10 shows the influence of the tire dimensionless numbers of each standing wave mode number on the modal tire model. As shown in Fig. 10, each tire dimensionless number has a dominant effect over a certain range of mode numbers. For example, R_s and T_s are dominant in low mode numbers, and B_s and C_w are dominant in high mode numbers. It means that the modal tire model is affected by all four tire model dimensionless numbers. It was verified that it is possible to accurately estimate four dimensionless numbers through standing wave characteristics.

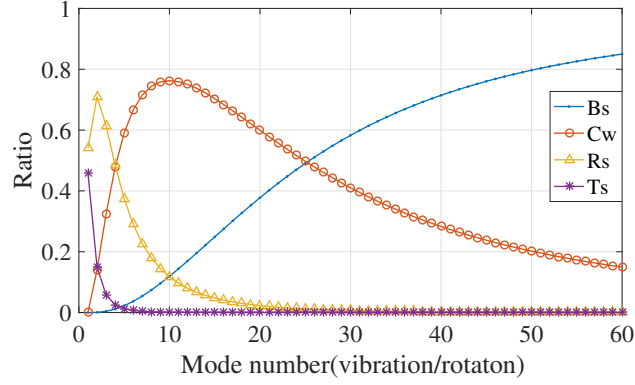


Figure 10: Influence of the dimensionless number of each standing wave mode number

Dimensionless number	Estimated value
Bending stiffness number ($= \frac{EI}{R^3 p_0} = \frac{bEh^3}{12r^4 p_0}$)	3.0833×10^{-3}
Contact width number ($= \frac{b}{R}$)	0.1953
Radial stiffness number ($= \frac{k_w}{p_0}$)	2.9740
Tangential stiffness number ($= \frac{k_v}{p_0}$)	2.5289

6. RESULTS

6.1. Estimation of tire dimensionless Numbers

In this section, the estimated values and the accuracy of the tire dimensionless numbers were analyzed. The x-axis of Fig. 11 represents the standing wave mode number and the y-axis represents the vibration amplitude of the standing wave in (27). The tire condition was 100% load, 65 km/h speed, 2.1 bar pressure, 0 mm wear.

In Fig. 11, the dotted line represents the measurement with intelligent tires, and the solid line represents the tire radial deformation based on the flexible ring tire model with estimated tire dimensionless numbers. It means that the standing wave characteristics are well represented through the proposed tire dimensionless numbers. The estimated tire dimensionless numbers are shown in Table. 3.

The radial acceleration of the tires through the estimated tire dimensionless numbers is shown in Fig. 12. The solid line represents the tire radial acceleration measured by the intelligent tire, and the dotted line represents the radial acceleration based on the flexible ring tire model with the estimated tire dimensionless numbers. This shows that the intelligent tire sensor signal can be described through only the four tire dimensionless numbers. And conversely, this means that it is possible to estimate the tire dimensionless numbers through the intelligent tire sensor signal.

6.2. Physical Meaning of tire dimensionless Numbers

In this section, the physical meaning of the newly defined four tire dimensionless numbers was analyzed. For each tire dimensionless number, the relationship with the tire condition dimensionless number was analyzed as shown in Fig. 13 - Fig. 16. The conditions of the intelligent tires used in the analysis are shown in Table. 1.

- Bending stiffness number(Bs) vs Wear number(Wn)

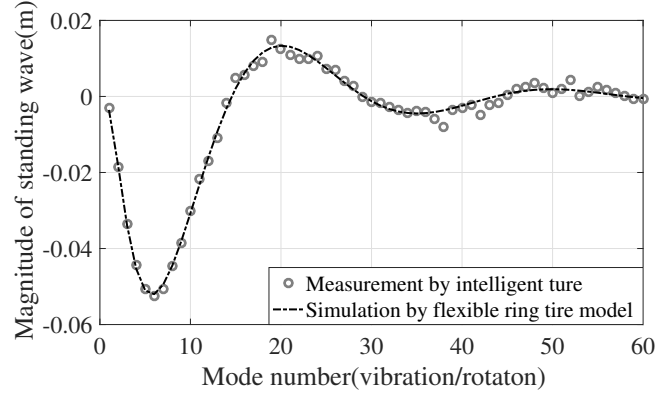


Figure 11: Estimated modal tire model standing wave characteristics

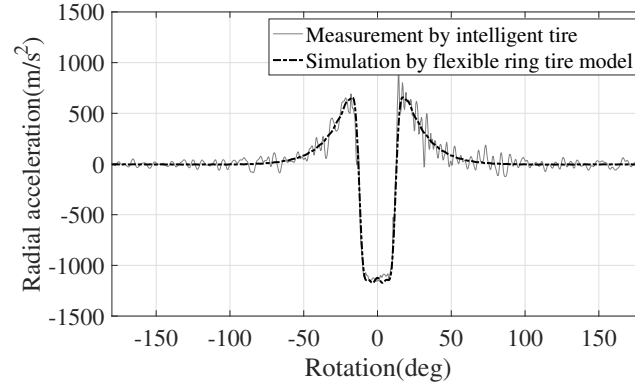


Figure 12: Radial acceleration signal of ring

A bending stiffness number is a dimensionless number of how well a tire bends. And it is proportional to h^3 as in (19). h is the tire tread depth, which represents the amount of tire wear. Therefore, the bending stiffness number will tend to decrease as h decreases, that is, as wear increases. This strategy has been verified by defining the wear number. Tire wear is expressed as the difference between the current tire thickness(h) and the initial tire thickness of the new tire(h_0). The wear number is defined as the tire wear divided by the tire radius as follows:

$$\text{Wear number} = \frac{\text{Amount of wear(mm)}}{\text{Tire radius(mm)}} = \frac{h_0 - h}{R} \quad (30)$$

Experiments were conducted on three wear-level tires (0mm, 2.9mm, 6.4mm). The relationship between bending stiffness number and wear number is shown in Fig. 13. As shown in the figure, the bending stiffness number decreases as the wear number increases.

This relationship between wear number and bending stiffness number is important in the field of tire wear. Tire wear is important information for vehicle safety. As the tire wears, the braking distance potentially increases by 30%. However, previous tire wear estimation has been studied based on mileage. That is the wear estimation algorithm is based on the tendency between wear and mileage. However, the mileage-based wear estimation algorithm is not robust to driving habits, weather, etc. And it has a disadvantage of accumulating estimation errors.

The proposed bending stiffness number can be used as a new wear estimation factor. Using the bending stiffness number as a tire wear estimation factor has several advantages. First, there is a constant tendency that the bending stiffness number decreases as tire wear increases. Second, estimation errors do not accumulate because it is possible to estimate the absolute value of tire wear. That is, it is possible to propose a new wear estimation algorithm based on

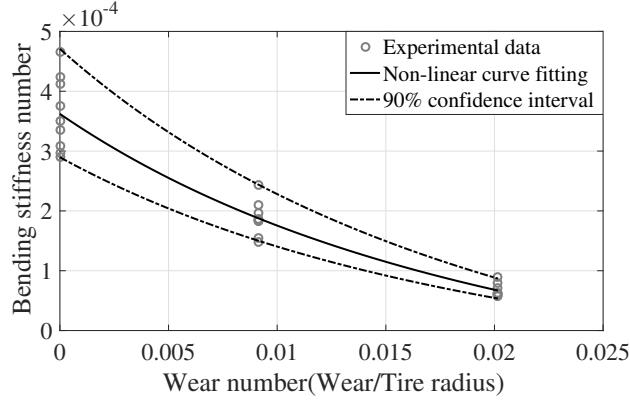


Figure 13: Bending stiffness number vs Wear number

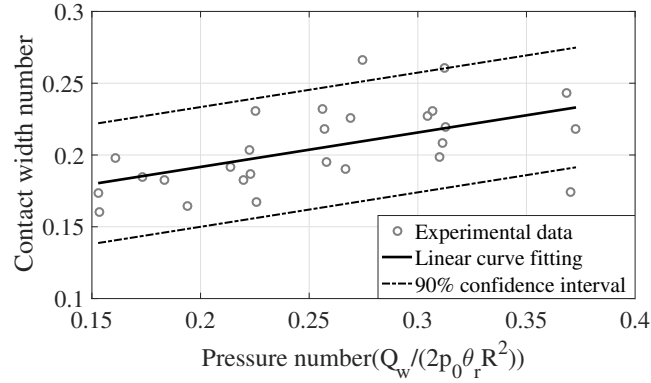


Figure 14: Contact width number vs Pressure number

the bending stiffness number.

In conclusion, the bending stiffness number represents the wear characteristics of the tire. Also, it is an important dimensionless number that can be used in the tire wear estimation algorithm.

- Contact width number(Cw) vs Pressure number(Pn)

The contact width number represents the ratio of the contact width to the tire radius. This contact width number was analyzed through correlation with the pressure number. The vertical force of a tire can be expressed simply as (31), assuming that the pressure (p_0) acts equally in the contact region. The pressure number can be derived as shown in (33).

$$Q_w \approx 2p_0bR\theta_r \quad (31)$$

$$\frac{b}{R} \approx \frac{Q_w}{2p_0\theta_r R^2} \quad (32)$$

$$\text{Pressure number} = \frac{Q_w}{2p_0\theta_r R^2} \quad (33)$$

The relationship between the contact width number and the pressure number is shown in Fig. 14. In this figure, the contact width number and the pressure number have a positive correlation, as in (32). This means that the larger the vertical force and the smaller the pressure, the larger the contact width. Also, for the same vertical force and pressure, the smaller the contact angle, the larger the contact width.

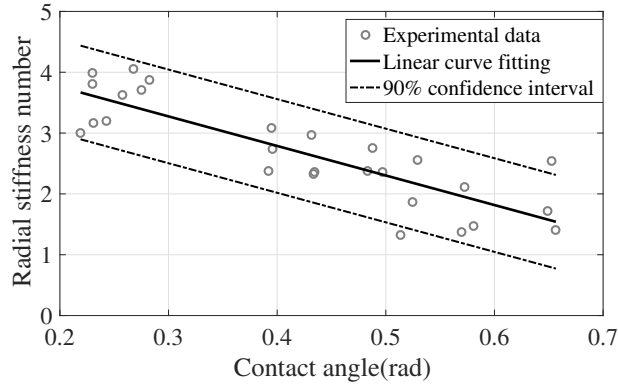


Figure 15: Radial stiffness number vs Contact angle

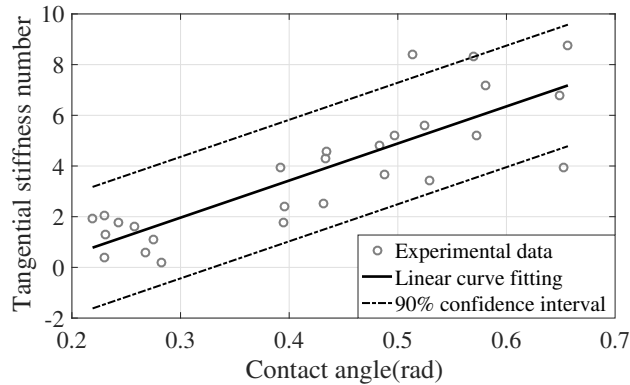


Figure 16: Tangential stiffness number vs Contact angle

The relationship between the contact width number and the pressure number is an important tire characteristic. If the force distribution is constant in the contact region, such as (31), the contact width number and pressure number should have a slope close to one. On the contrary, the farther the slope is from one, the less uniform the tire force distribution. The relationship between these two dimensionless numbers can be used as important information to determine the contact characteristics of the tire.

The estimated contact width number has its significance. Tire contact width is an important tire characteristic in vehicle control. Larger tire contact width increases grip characteristics and cornering stiffness during lateral motion. It means, making it easier to secure vehicle control. However, there are disadvantages in terms of vehicle responsiveness. That is, the tire contact width has a trade-off relationship in terms of vehicle control and vehicle responsiveness. In previous studies, the tire contact width has been estimated from the tire footprint [23], [24]. The use of the proposed contact width number has the advantage that it is easy to estimate and analyze the tire contact width through intelligent tires.

- Radial stiffness number(R_s), Tangential stiffness number(T_s) vs Contact angle

Physically, the radial stiffness number and the tangential stiffness number represent the relationship of tire sidewall stiffness to pressure. In tire characteristics, the radial stiffness and tangential stiffness of the tire sidewall are important factors to determine the deformation and contact property of the tire. However, since tire sidewalls are made of composite materials, there are many limitations in measuring or estimating radial stiffness and tangential stiffness. Using the proposed tire dimensionless number estimation algorithm, the radial stiffness and tangential stiffness can be easily estimated.

The sidewall stiffness varies with tire condition. In the previous study, the sidewall stiffness relationship for pressure and sidewall angle has been analyzed [35]. In a previous study, the tire sidewall stiffness is expressed as a function of sidewall angle and pressure. However, it has limitations that are difficult to verify experimentally and require offline analysis. The proposed radial/tangential stiffness numbers make it possible to analyze sidewall stiffness characteristics in real-time.

In this paper, the contact angle is selected as the dimensionless number of comparisons between the radial stiffness number and the tangential stiffness number. Since the contact angle value includes pressure and sidewall angle information, the relationship between the contact angle and radial/tangential stiffness numbers represents the characteristics of the tire.

The tendency of the radial stiffness number to the contact angle is shown in Fig. 15. The tendency of the tangential stiffness number for the contact angle is shown in Fig. 16. The radial stiffness number decreases with increasing contact angle, and the tangential stiffness number increases with increasing contact angle. For the tire used in this study, we can analyze that the radial stiffness dominates when the contact angle is small and the tangential stiffness dominates when the contact angle is large. In conclusion, the proposed radial / tangential stiffness number makes it easy to analyze the tire sidewall characteristics. This means that the tire sidewall characteristics analysis, which was very difficult experimentally, can be easily analyzed through intelligent tires.

In this section, we verified that the proposed tire dimensionless number estimation algorithm has several advantages. First, the proposed tire dimensionless numbers well describe the standing wave and signal characteristics of radial acceleration. Also, intelligent tire sensor signals can be analyzed based on the physical tire model. Second, tire dimensionless numbers can be estimated through intelligent tire sensor signals. The estimated tire dimensionless numbers can be used to analyze tire characteristics. Finally, the tendency of tire dimensionless numbers for various tire state dimensionless numbers was analyzed. This has the advantage that the characteristics of tires can be analyzed easily and quickly compared to previous tire characteristics studies.

7. CONCLUSION

In this paper, the physical model with the tire dimensionless numbers is introduced. The complex flexible ring tire model was simplified through modal analysis. The proposed tire dimensionless numbers represent a simplified model. Each tire dimensionless number was named bending stiffness number (B_s), contact width number (C_w), Radial stiffness number (R_s), and tangential stiffness number (T_s). An algorithm for estimating tire dimensionless numbers using an intelligent tire sensor signal has been proposed. The proposed estimation algorithm has been verified by several experiments. The tire dimensionless numbers have been compared with tire condition dimensionless numbers. As a result, it was confirmed that the proposed tire dimensionless number represents well the characteristics of the tire and the intelligent tire signal. Intelligent tire signal analysis based on tire model dimensionless numbers has the following advantages: First, the generality and robustness of intelligent tire research can be guaranteed. The tire dimensionless numbers can be used to explain and analyze previous data-based intelligent tire researches. It can also be used as a powerful feature in the field of machine learning of intelligent tire signals. Secondly, it is possible to identify tire characteristics that are not easily known experimentally. Based on the proposed algorithm, it is possible to analyze and monitor sidewall stiffness and contact characteristics according to tire conditions such as temperature and aging. In conclusion, the proposed tire dimensionless number and characteristic analysis are expected to contribute to the field of tire research, vehicle control, and measurement.

Acknowledgment

This research was partly supported by the Industrial Strategic Technology Development Program funded by the HANKOOK TIRE CO.LTD., the BK21+ program through the NRF funded by the Ministry of Education of Korea, the Technology Innovation Program (20010263, Development of innovative design for UX environment improvement and commercialization model of wheelchair electric motorization kit with enhanced portability and convenience) funded By the Ministry of Trade, Industry Energy(MOTIE, Korea), and the National Research Foundation of Korea(NRF) grant funded by the Korea government(MSIP) (No. 2020R1A2B5B01001531).

References

- [1] M. Doumiati, A. C. Victorino, A. Charara, D. Lechner, Onboard real-time estimation of vehicle lateral tire–road forces and sideslip angle, *IEEE/ASME Transactions on Mechatronics* 16 (4) (2010) 601–614.
- [2] J.-w. Yoon, B.-w. Kim, Vehicle position estimation using nonlinear tire model for autonomous vehicle, *Journal of Mechanical Science and Technology* 30 (8) (2016) 3461–3468.
- [3] J. Subosits, J. C. Gerdes, Autonomous vehicle control for emergency maneuvers: The effect of topography, in: 2015 American Control Conference (ACC), IEEE, 2015, pp. 1405–1410.
- [4] Z. Liu, Q. Gao, H. Niu, In-plane flexible beam on elastic foundation with combined sidewall stiffness tire model for heavy-loaded off-road tire, *Journal of Dynamic Systems, Measurement, and Control* 141 (6) (2019).
- [5] R. Marsili, Measurement of the dynamic normal pressure between tire and ground using pvdf piezoelectric films, *IEEE Transactions on Instrumentation and Measurement* 49 (4) (2000) 736–740.
- [6] J. Ejsmont, W. Owczarzak, Engineering method of tire rolling resistance evaluation, *Measurement* 145 (2019) 144–149.
- [7] F. Braghin, M. Brusarosco, F. Cheli, A. Cigada, S. Manzoni, F. Mancosu, Measurement of contact forces and patch features by means of accelerometers fixed inside the tire to improve future car active control, *Vehicle System Dynamics* 44 (sup1) (2006) 3–13.
- [8] A. Niskanen, A. Tuononen, Three three-axis ipep accelerometers on the inner liner of a tire for finding the tire-road friction potential indicators, *Sensors* 15 (8) (2015) 19251–19263.
- [9] R. Matsuzaki, N. Hiraoka, A. Todoroki, Y. Mizutani, Analysis of applied load estimation using strain for intelligent tires, *Journal of Solid Mechanics and Materials Engineering* 4 (10) (2010) 1496–1510.
- [10] H. Lee, S. Taheri, Intelligent tires? a review of tire characterization literature, *IEEE Intelligent Transportation Systems Magazine* 9 (2) (2017) 114–135.
- [11] H. Morinaga, Method for estimating tire wear and apparatus for estimating tire wear, uS Patent 8,483,976 (Jul. 9 2013).
- [12] Y. Hanatsuka, Method and apparatus for detecting wear of tire, uS Patent 8,061,191 (Nov. 22 2011).
- [13] D. Krier, G. S. Zanardo, L. del Re, A pca-based modeling approach for estimation of road-tire forces by in-tire accelerometers, *IFAC Proceedings Volumes* 47 (3) (2014) 12029–12034.
- [14] H. Y. Jo, M. Yeom, J. Lee, K. Park, J. Oh, Development of intelligent tire system, Tech. rep., SAE Technical Paper (2013).
- [15] D. Jeong, S. Kim, J. Lee, S. B. Choi, M. Kim, H. Lee, Estimation of tire load and vehicle parameters using intelligent tires combined with vehicle dynamics, *IEEE Transactions on Instrumentation and Measurement* 70 (2020) 1–12.
- [16] S. Hong, J. K. Hedrick, Tire-road friction coefficient estimation with vehicle steering, in: 2013 IEEE Intelligent Vehicles Symposium (IV), IEEE, 2013, pp. 1227–1232.
- [17] S. Hong, G. Erdogan, K. Hedrick, F. Borrelli, Tyre–road friction coefficient estimation based on tyre sensors and lateral tyre deflection: modelling, simulations and experiments, *Vehicle system dynamics* 51 (5) (2013) 627–647.
- [18] G. Erdogan, S. Hong, F. Borrelli, K. Hedrick, Tire sensors for the measurement of slip angle and friction coefficient and their use in stability control systems, *SAE International Journal of Passenger Cars-Mechanical Systems* 4 (2011-01-0095) (2011) 44–58.
- [19] G. Erdogan, L. Alexander, R. Rajamani, A novel wireless piezoelectric tire sensor for the estimation of slip angle, *Measurement Science and Technology* 21 (1) (2009) 015201.
- [20] X. Yang, O. Olatunbosun, D. Garcia-Pozuelo, E. Bolarinwa, Fe-based tire loading estimation for developing strain-based intelligent tire system, Tech. rep., SAE Technical Paper (2015).
- [21] J. Wu, Z. Wang, Z. Zhao, Influence of tire inflation pressure on vehicle dynamics and compensation control on fwid electric vehicles, *Journal of Dynamic Systems, Measurement, and Control* 142 (7) (2020).
- [22] J. Goos, A. Teerhuis, A. Schmeitz, I. Besselink, H. Nijmeijer, Model-based state estimator for an intelligent tire, in: 13th International Symposium on Advanced Vehicle Control (AVEC 2016), CRC Press/Balkema, 2017, pp. 503–508.
- [23] J. Löwer, P. Wagner, H. Unrau, C. Bederna, F. Gauterin, Dynamic measurement of the fluid pressure in the tire contact area on wet roads, *Automotive and Engine Technology* (2020) 1–8.
- [24] P. Farhadi, A. Golmohammadi, A. Sharifi, G. Shahgholi, Potential of three-dimensional footprint mold in investigating the effect of tractor tire contact volume changes on rolling resistance, *Journal of Terramechanics* 78 (2018) 63–72.
- [25] A. Soltani, A. Goodarzi, M. H. Shojaeefard, K. Saeedi, Optimizing tire vertical stiffness based on ride, handling, performance, and fuel consumption criteria, *Journal of Dynamic Systems, Measurement, and Control* 137 (12) (2015).
- [26] S. Kim, P. E. Nikravesh, G. Gim, A two-dimensional tire model on uneven roads for vehicle dynamic simulation, *Vehicle system dynamics* 46 (10) (2008) 913–930.
- [27] A. Gasmi, P. F. Joseph, T. B. Rhyne, S. M. Cron, Development of a two-dimensional model of a compliant non-pneumatic tire, *International Journal of Solids and Structures* 49 (13) (2012) 1723–1740.
- [28] F. Ballo, M. Gobbi, G. Mastinu, G. Previati, Motorcycle tire modeling for the study of tire–rim interaction, *Journal of Mechanical Design* 138 (5) (2016) 051404.
- [29] K. Yamagishi, J. Jenkins, Singular perturbation solutions of the circumferential contact problem for the belted radial truck and bus tire, *Journal of Applied Mechanics* 47 (3) (1980) 519–524.
- [30] S. Gong, Study of in-plane dynamics of tires (1993).
- [31] S.-J. Kim, A. R. Savkoor, The contact problem of in-plane rolling of tires on a flat road, *Vehicle System Dynamics* 27 (S1) (1997) 189–206.
- [32] Z.-X. Yu, H.-F. Tan, X.-W. Du, L. Sun, A simple analysis method for contact deformation of rolling tire, *Vehicle System Dynamics* 36 (6) (2001) 435–443.
- [33] A. J. Niskanen, Y. Xiong, A. J. Tuononen, Towards the friction potential estimation: A model-based approach to utilizing in-tyre accelerometer measurements, in: 2016 IEEE Intelligent Vehicles Symposium (IV), IEEE, 2016, pp. 625–629.
- [34] E. Buckingham, On physically similar systems; illustrations of the use of dimensional equations, *Physical review* 4 (4) (1914) 345.
- [35] M. Matsubara, D. Tajiri, M. Horiuchi, S. Kawamura, Evaluation of spring properties of tire sidewall under changes in inflation pressure, *SAE International Journal of Passenger Cars-Mechanical Systems* 8 (2015-01-2193) (2015) 825–833.